Preparation of Flame-Retardant Cellulose Paper *via* Spray Coating with Lignin, Phytic Acid, and Sodium Silicate

Soon Wan Kweon, Yong Ju Lee, Tai-Ju Lee,* and Hyoung Jin Kim *

* *Corresponding authors: leetj@kookmin.ac.kr, hyjikim@kookmin.ac.kr*

DOI: 10.15376/biores.20.2.3808-3825

GRAPHICAL ABSTRACT

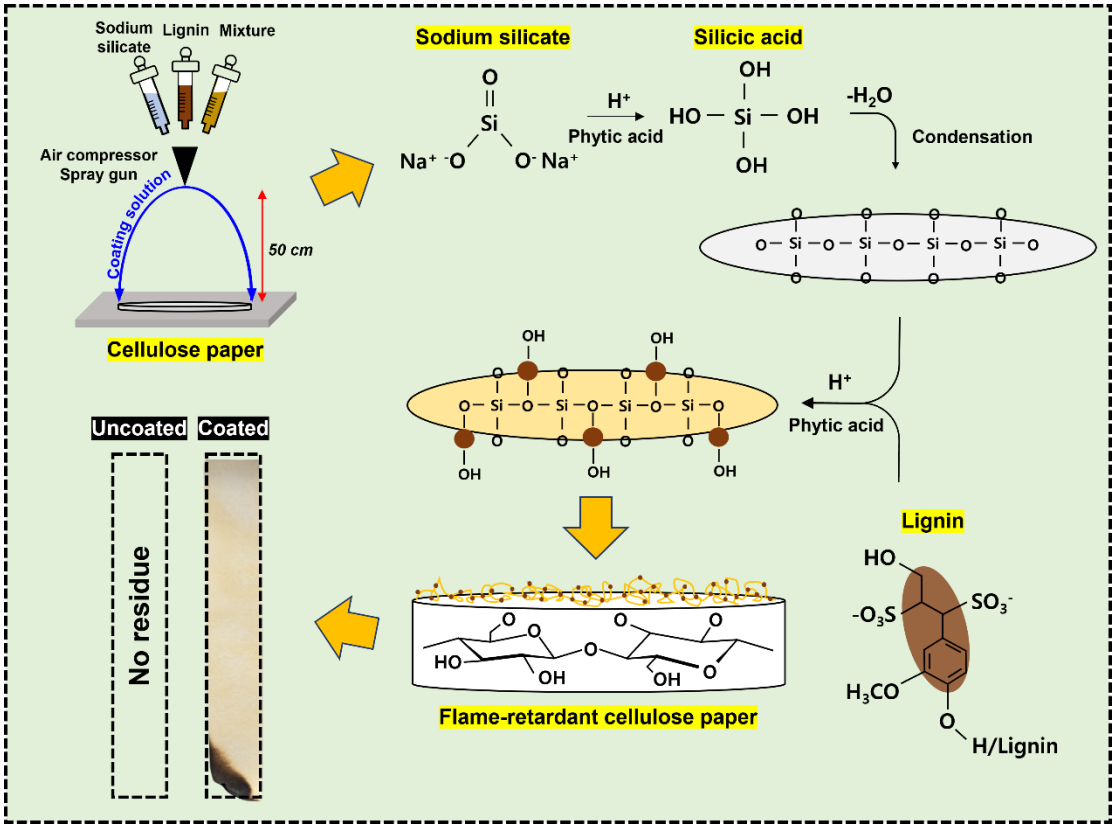

Preparation of Flame-Retardant Cellulose Paper *via* Spray Coating with Lignin, Phytic Acid, and Sodium Silicate

Soon Wan Kweon, Yong Ju Lee, Tai-Ju Lee,* and Hyoung Jin Kim *

A flame-retardant treatment for cellulosic paper was applied by spraying the paper with combinations of lignin, phytic acid, and sodium silicate. Lignin enhanced the flame retardancy in the condensed phase, while phytic acid provided dual-phase flame resistance. Sodium silicate further improved thermal stability by forming silica gel through its reaction with phytic acid. The limiting oxygen index increased from 16.8% to 22.0%, and in vertical flame tests, treated paper self-extinguished within 1.5 s, whereas untreated paper burned completely in 12.0 s. Thermogravimetric analysis revealed enhanced thermal stability, with treated paper retaining 36.5% residual char at 900 °C compared to 0% in untreated paper. Despite the relatively low coating coverage from the spray deposition method, the synergistic interaction of phytic acid, lignin, and silica gel effectively compensated by promoting dense char formation and thermal insulation. Fire retardancy was attributed to phytic acid-catalyzed lignin and silica composite formation in the char layer, enhancing structural stability and shielding efficiency. Raman spectroscopy confirmed improved graphitization (I_D/I_G = 1.20), while scanning electron microscopy with energy dispersive X-ray spectroscopy (SEM-EDX) and Fourier transform infrared spectroscopy (FT-IR) verified phosphorus and silica retention. This treatment showed potential for high-performance flame-retardant cellulose materials in packaging, construction, and other industries.

DOI: 10.15376/biores.20.2.3808-3825

Keywords: Cellulose; Flame retardancy; Condensed phase; Gas phase; Spray coating; Self-extinguishing; Sulfonated kraft lignin; Sodium silicate; Silica gel

Contact information: Department of Forest Products and Biotechnology, Kookmin University, 77 Jeongneung-ro, Seongbuk-gu, Seoul 02707 Republic of Korea;
** Corresponding authors: leetj@kookmin.ac.kr, hyjikim@kookmin.ac.kr*

INTRODUCTION

Cellulose derived from wood is the most abundant natural polymer (Figueiredo *et al*. 2010). Wood-based cellulose has served as a primary raw material in the pulp and paper industry, contributing to the production of biodegradable, recyclable, and cost-effective paper materials (Laftah and Wan 2016). However, the highly flammable nature of cellulosic fibers hinders their broad application (Saba *et al*. 2016). Paper-based products show high flammability even after the incorporation of flame-retardant additives into the bulk of the fiber wall, either during the paper-making process or as a posttreatment of paper (Köklükaya *et al*. 2015). The most widely used flame-retardant additives contain elements such as phosphorus and halogens or inorganic compounds such as silicates, hydroxides, and hydrotalcites (Nassar *et al*. 1999; Katović *et al*. 2009; Zheng *et al*. 2019; Jeong *et al*. 2022). Generally, the flame retardancy of polymeric materials can be improved through the incorporation of various flame-retardant systems that act in the condensed phase, gas phase, or both. Figure 1 shows the mechanisms of flame retardance in the condensed and gas phases. In the condensed phase, flame retardants function by forming a thermally insulating char layer to protect the

underlying material from fire. This char layer acts as a barrier, inhibiting the transmission of heat to the underlying polymer matrix. It also retards the release of combustible gases, which act as fuels in the combustion zone, during degradation (Yang *et al*. 2020).

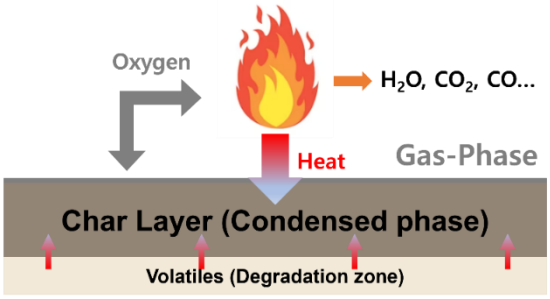

Fig. 1. Combustion model for a flame-retardant material

Lignin, an abundant polyphenolic compound derived from biomass, particularly plant fibers, has garnered considerable interest in multiple areas. It possesses notable thermal stability, with a peak degradation temperature of approximately 350 °C in a nitrogen atmosphere (Costes *et al*. 2017). The degradation temperature of lignin can vary depending on several factors, including its molecular weight, functional group composition, and the presence of linkages such as β–O–4 ether bonds, which are more susceptible to thermal cleavage (Fan *et al.* 2017; Prieur *et al.* 2017). Additionally, its aromatic chemical structure contributes to a high char yield after decomposition, which reaches approximately 40% at 900 °C (Ferry *et al*. 2015). These properties make lignin a promising flame-retardant additive. At 250 °C, weak bonds such as the β–O–4 ether linkages in lignin are cleaved, and phenolic radicals are continuously produced. These phenolic radicals may further fragment to form other small compounds or radicals or participate in repolymerization via free-radical reactions (Fan *et al*. 2017). At the same time, the cleaving of strong bonds in lignin, such as the C–C bonds, with the removal of most functional groups results in the carbonization of the remaining aromatic rings in the char and the formation of a condensed ring network (Mousavioun *et al*. 2010; Song *et al*. 2011; Bertini *et al*. 2012; Ferry *et al*. 2017; Zhang *et al*. 2021). Flame-retardant effects in the gas phase are realized through the generation of active species that can act as free-radical scavengers in the combustion zone (Yang *et al*. 2020). In particular, polymeric materials such as halogen- or phosphorus-containing compounds can interrupt the combustion reaction of flammable volatiles in the gas phase.

Phytic acid (PA) is a phosphate-rich compound primarily derived from nuts, oilseeds, and cereals, where it serves as the main storage form of phosphorus in plant seeds, playing a crucial role in seed development and germination by providing essential nutrients (Reddy *et al.* 1982; Graf and Eaton 1990). It consists of six phosphate groups attached to a six-carbon ring, as shown in Fig. 2. In the condensed phase, PA produces a flame-retardant effect through two key mechanisms. First, acids generated during the pyrolysis of PA facilitate the swift dehydration and carbonization of oxygen-containing polymeric materials, resulting in the formation of a dense coke layer. This coke layer acts as an effective barrier, inhibiting the release of oxygen, heat, and volatile combustible gases. Second, PA transforms into polyphosphoric acid, which is a highly thermally stable and nonvolatile flame-retardant material. Polyphosphoric acid covers the surface of the polymer material, promoting the consolidation of the carbon layer and further improving flame retardance (Kong *et al*. 2020; Yuan *et al*. 2021; Zhang *et al*. 2021; Liu *et al*. 2023). In the gas phase, PA decomposes and generates phosphorus-containing radicals, such as HPO−, PO−, and HPO_2−. These radicals can scavenge

reactive HO and H radicals formed during the combustion of the polymeric material, suppressing the combustion chain reaction and thereby reducing the flammability of the substrate (Liu *et al*. 2018; Cheng *et al*. 2020; Liu *et al*. 2023).

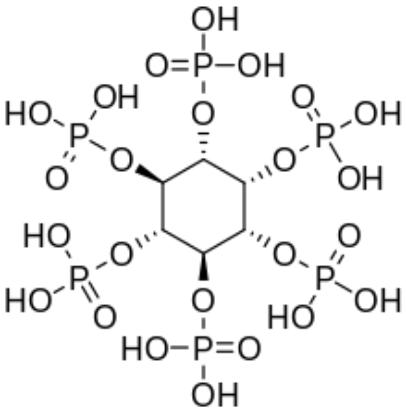

Fig. 2. Structural formula of phytic acid

Inorganic silica (SiO_2), known for its distinctive layered structure, is abundantly available in nature and has a chemical structure allowing intercalation. This makes it an economically advantageous material for the production of polymer nanocomposites. SiO_2 is commonly synthesized from a sodium silicate (Na_2SiO_3, water glass) precursor solution *via* the sol–gel method, which requires an acid (Niu *et al*. 2014). Low pH results in the formation of silicic acid, which further condensates/polymerizes to form a solid SiO_2 gel (Lin *et al*. 2023). Additionally, it has been found that the presence of silicon in flame retardants can improve the thermal stability of the char layer formed during combustion (Ni *et al*. 2011).

Studies on the manufacturing of eco-friendly flame-retardant composite materials have been steadily increasing in number in recent years. Liu *et al*. (2018) enhanced the flame resistance of lyocell fibers through the application of PA–ammonium, resulting in an increase in the limiting oxygen index (LOI) value. Xu *et al*. (2019) explored the flame-retardant properties of ammonium phosphite-treated paper, reporting a reduction in char length from 210 to 45 mm. Furthermore, thermogravimetric analysis (TGA) revealed that the treated samples had a lower initial decomposition temperature and yielded more residue than the untreated samples. Chen *et al*. (2021) utilized PA modified with dicyandiamide to improve the flame retardancy of cellulosic paper. Notably, at a concentration of the modified PA of 20%, the char length of the paper decreased from 12.5 to 4.1 cm, accompanied by a remarkable increase in the LOI value, from 19.6% to 41.5%. In other studies, Li *et al*. (2019) examined flame-retardant wood nanofibers containing lignin, and Lin *et al*. (2023) investigated the potential of a PA–silica hybrid system as a flame retardant.

The objective of the present study was to impart flame retardance to paper by spray coating it with a system prepared from lignin, PA, and sodium silicate. Specifically, this study investigates how PA facilitates the formation of thermally stable silica gels from sodium silicate and how this process, in conjunction with the char-forming properties of lignin, contributes to flame retardance. By clarifying these mechanisms, the present work provides a novel approach to integrating bio-based and inorganic components for the development of sustainable and efficient flame-retardant solutions.

EXPERIMENTAL

Materials

The Quantitative filter paper (mass per unit area: 80 g/m²) obtained from Hangzhou Whatman-Xinhua Filter Paper Co., Ltd. (China) was used as base paper. All the paper samples were dried at 105 °C for 24 h before use. Filter paper was selected because other types of wood pulp contain small amounts of lignin, which forms a lignin matrix. In such cases, it is challenging to effectively embed flame-retardant polymers within the fiber structure (Kalia *et al*. 2011; Li *et al*. 2019).

Sulfonated kraft lignin (average M_w ~10,000, 4% sulfur, pH 10.5, soluble in water, particle size 125 to 180 μm) was purchased from Sigma-Aldrich (Stockholm, Sweden). Sulfonated kraft lignin is produced through a hot alkaline (sulfate) process and then modified *via* sulfonation. A 50% (w/w) aqueous solution of PA was also purchased from Sigma-Aldrich. Technical-grade aqueous solution of sodium silicate (27.6% SiO_2 and 8.5% Na_2O) was acquired from Daejung Chemical Co. (Republic of Korea).

Preparation of the Flame-Retardant Paper

The flame-retardant coating solution was diluted to a concentration of 10% with deionized water and spray-coated on both sides of the base paper 15 times, as shown in Fig. 3. Table 1 lists the compositions of the coating solutions. The control sample that was not spray-coated was named C, the sample treated only with sodium silicate was named S, the sample treated only with lignin was named L, the sample treated with lignin and PA was named LP, and the sample treated with PA and sodium silicate was named PS. The sample named LPS was prepared through a sequential spray-coating process, involving an initial coating of lignin followed by a separate coating with a mixture of phytic acid and sodium silicate. This method was designed to promote optimal interaction between the components, enhancing the synergistic flame-retardant effect.

The compositions of the flame-retardant coating solutions were determined in advance based on the pH of the mixture, to maintain the pH at 6.5 to 7.0. In the preliminary experiment, where the paper was treated only with PA, the strength of the sheet decreased, and it became brittle because of the acidity of PA. The coated papers were dried at 110 °C for 5 min using an automatic sheet press (HANTECH, Korea) at a pressure of 410 ± 10 kPa. The manufacturing process employed herein for the production of flame-retardant paper is schematically shown in Fig. 3.

Table 1. Formulations of Flame-Retardant Coatings

Code	Composition of the Coating Solutions (wt.%)			Coating Weight (g/m^2)
	Lignin	Phytic acid	Sodium silicate	
C	-	-	-	-
S	-	-	10.00	4.5 ± 0.67
L	10.00	-	-	8.0 ± 0.34
LP	9.50	0.50	-	8.3 ± 0.04
PS	-	6.65	3.35	5.3 ± 0.87
LPS*	10.00	-	-	10.5 ± 0.79
	-	6.65	3.35	

* two-step (L, PS) process employed

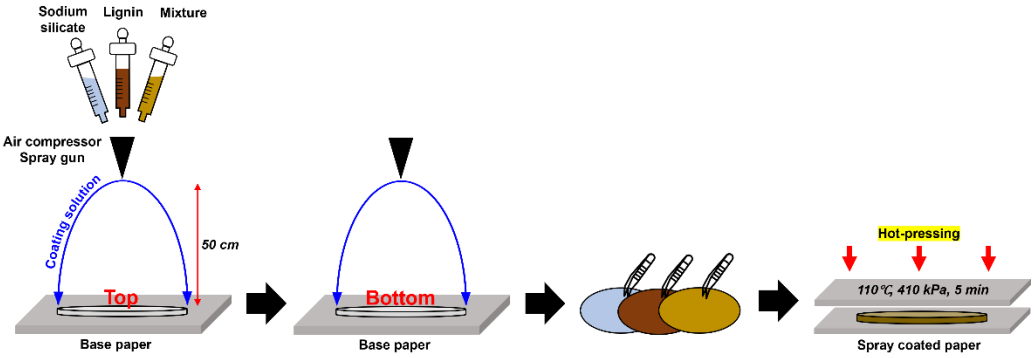

Fig. 3. Schematic of the manufacturing of flame-retardant paper

Characterization and Tests

Flammability test

Herein, flame retardance was evaluated using LOI and UL-94 tests. LOI is defined as the minimum oxygen concentration (vol%) required to sustain the continuous combustion of a material in a flowing mixture of oxygen and nitrogen for 3 min or until 5 cm of the sample is consumed (Yang *et al*. 2020). The LOI value was calculated using Eq. 1. In the LOI test, the sample was positioned vertically at the center of a glass chimney and ignited with a burner placed above the sample. Five tests were performed for each sample type to obtain reliable results. A higher LOI value indicates better flame retardance.

$$\text{LOI} = \frac{[O_2]}{[O_2]+[N_2]} \text{ X } 100\ \% \quad (1)$$

The vertical flame test was conducted according to the ASTM D 3801–19 standard, which aligns with the UL-94 test method for evaluating the flammability of materials. The vertical flammability test is commonly used for evaluating the flammability of paper (Chen *et al*. 2021). In particular, the UL-94 vertical burning test is the most frequently used test for measuring the ignitability and flame spread of materials (Yang *et al*. 2020). Herein, samples were tested according to an international standard, IEC 60695-11-10 (2013), with five tests performed in parallel. The samples used for this test had dimensions of 125 mm × 13 mm. In the results of this test, afterflame time indicates the duration of flame application, and afterglow time is the duration required for the fire glow to completely disappear.

Scanning electron microscopy (SEM)-energy dispersive x-ray (EDX) analysis

The surface morphologies and the elemental distribution of the uncoated reference and spray-coated paper samples were observed using SEM-EDX (JSM 7401F, JEOL Ltd., Japan) after sputtering with Pt. The acceleration voltage of the electron beam was set to 5 kV for SEM and 10 kV for EDX.

Thermogravimetric analysis (TGA)

The thermal stabilities of the uncoated reference and spray-coated paper samples were investigated using TGA (Perkin Elmer TGA8000TM, USA). The sample mass was 5 g, and the measurements were performed at a constant heating rate of 20 °C/min from 40 °C to 900 °C in N_2 supplied at a flow rate of 20 mL/min. The differential thermogravimetry (DTG) curves were obtained from TGA curves using R software (R Core Team, ver. 4.3.0, Auckland, New Zealand), with smoothing performed using a smoothing algorithm.

Attenuated total reflection infrared (ATR-IR) spectroscopy

The chemical structures of the uncoated reference and spray-coated insulating materials were investigated using ATR-IR spectroscopy (Nicolet iS50, Thermo Fisher Scientific, USA). Each spectrum was recorded in the range of 4,000 to 400 cm^{-1} at a resolution of 4 cm^{-1}, employing 32 scans. The absorption of air was recorded and used as the reference standard.

Raman spectroscopy analysis

The char residues of the uncoated reference and spray-coated insulating materials were determined using Raman spectroscopy (LabRam Soleil, HORIBA Scientific, France). Each spectrum was obtained in the backscattering geometry configuration using a 532 nm argon laser in the scan range of 300 to 3000 cm^{-1}.

RESULTS AND DISCUSSION

Flame-Retardant Behavior Analysis

Flammability analysis

Figure 4 shows the measured LOI. LOI has been considered an important indicator of the flammability of paper (Xu *et al*. 2019; Chen *et al*. 2021; Liu *et al*. 2022). A higher LOI value indicates a higher O_2 concentration required to sustain combustion, suggesting higher fire resistance (Martinka *et al*. 2022). According to the results, the LOI of sample C was 16.8%, whereas coated samples showed higher LOI values. Sample LPS exhibited the highest LOI value (22.0%), suggesting the best flame resistance of this sample under a small flame scenario.

Although the LPS sample demonstrated superior flame retardancy, additional analysis revealed that the total coating weight (Table 1) alone did not directly correlate with the LOI values (R^2 = 0.42), indicating that the enhanced performance was primarily due to the synergistic effect of the combined flame-retardant components rather than the total mass of applied material. This synergistic interaction contributed significantly to the improved flame resistance, highlighting the importance of the chemical composition and component interaction rather than coating weight alone. This observation emphasizes that achieving optimal flame retardancy requires a well-designed combination of functional additives rather than relying solely on increasing coating mass.

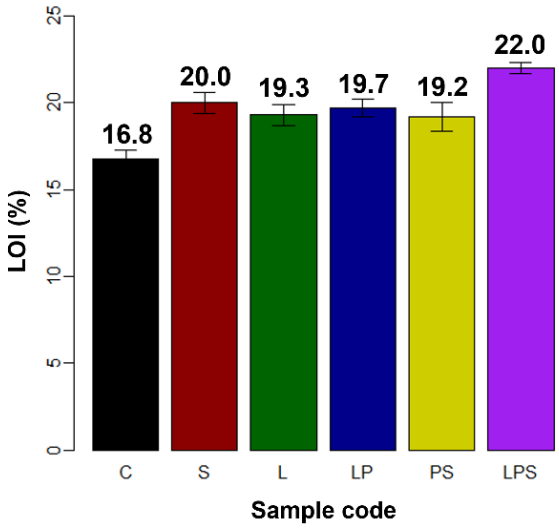

Fig. 4. Limiting oxygen index values of the paper samples

Table 2 shows the results of the vertical flammability test, listing both afterflame time and afterglow time. For both parameters, a shorter time indicates better flame retardance.

As shown in Table 2, the reference sample C completely burned when ignited in air. Samples S and L, coated with single materials, showed better flame resistance than sample C but still exhibited low flame retardance. Samples PS and LPS, coated with two or more materials, showed improved flame resistance. In particular, sample LPS exhibited a very short afterflame time and no afterglow time, indicating a considerably decreased combustion rate and excellent flame retardance. At the same time, sample LP did not self-extinguish after ignition. This was attributed to the relatively low availability of PA, resulting in a weak gas-phase flame-retardant effect. These results suggest that achieving excellent flame retardance likely requires a synergetic effect in both the gas and condensed phases (Yang *et al*. 2020).

Table 2. Results of the Vertical Flammability Test of the Paper Samples

Code	Time (seconds)		Dripping
	Afterflame	Afterglow	
C	12.0	-	Yes
S	7.7	37.5	No
L	8.1	17.3	Yes
LP	10.7	16.7	Yes
PS	4.4	1.8	No
LPS	1.5	0.0	No

Figures 5 and 6 show digital photographs of the samples during and after the vertical flammability test, respectively. Upon exposure to flame, the uncoated sample C burned rapidly and completely, without any residual char residue. At the same time, sprayed samples exhibit notably lower rate and degree of combustion. The combustion degree was analyzed using the Free Form function in the image processing and analysis software PicMan (WaferMasters, Inc., Dublin, CA, USA). As a result, samples PS and LPS show degrees of combustion lower by approximately 95.3% and 97.4%, respectively, than the untreated sample C.

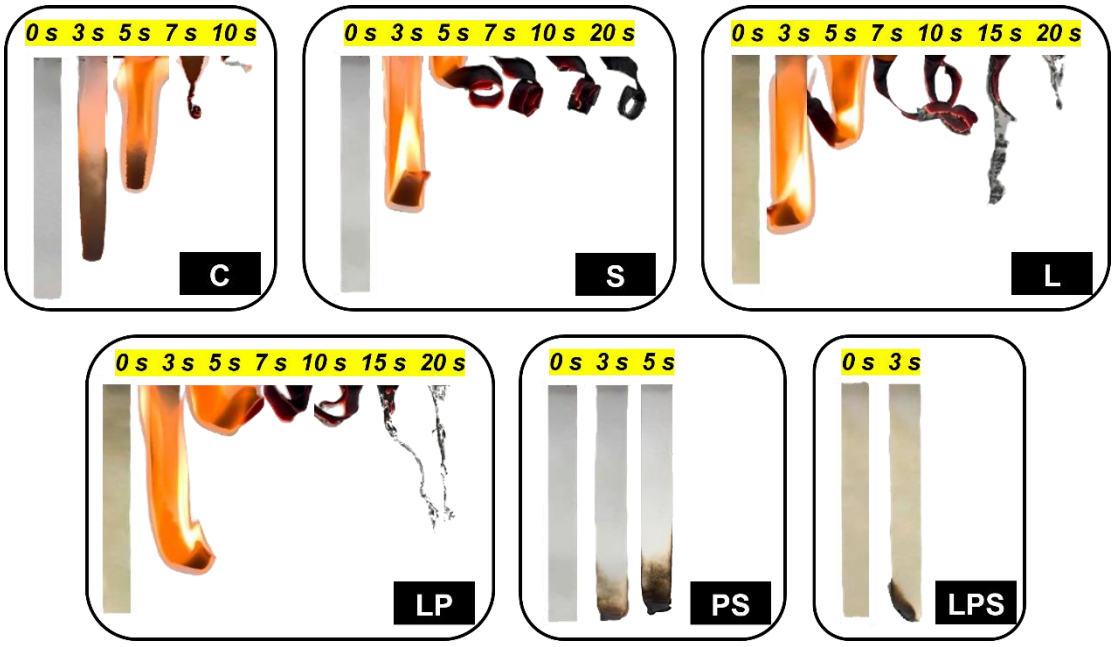

Fig. 5. Combustion behavior of paper samples

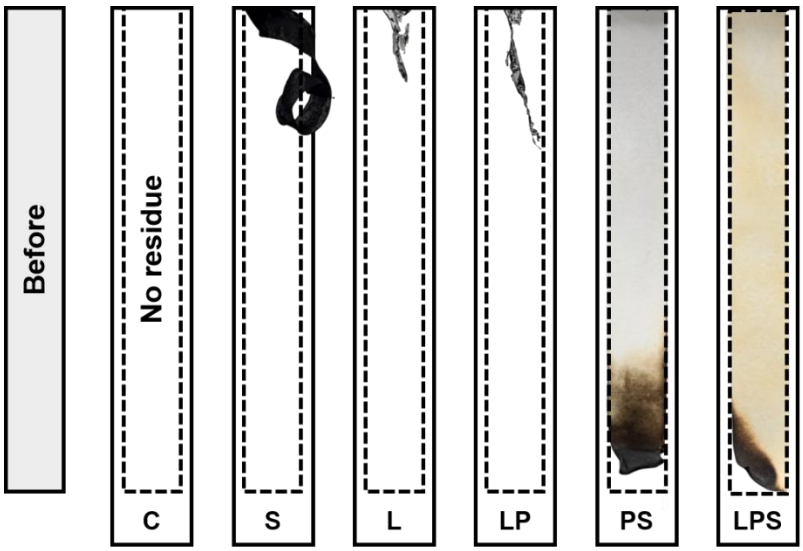

Fig. 6. Digital photographs of paper samples after UL-94 burning tests

Surface Morphology Analysis

The SEM images of samples C, PS, and LPS are shown in Fig. 7. At elevated temperatures, PA releases phosphorous/polyphosphate, which accelerates the carbonization of the fiber matrix and forms a protective char layer (Liu *et al*. 2023). Additionally, the reduction in pH facilitates the conversion of sodium silicate into silicic acid (Niu *et al*. 2014; Schlomach and Kind 2004), which subsequently polymerizes into a robust silica network. This silica gel is not only deposited on the fiber surface but also infiltrates the interior of the fiber network, reinforcing the structural integrity of the material.

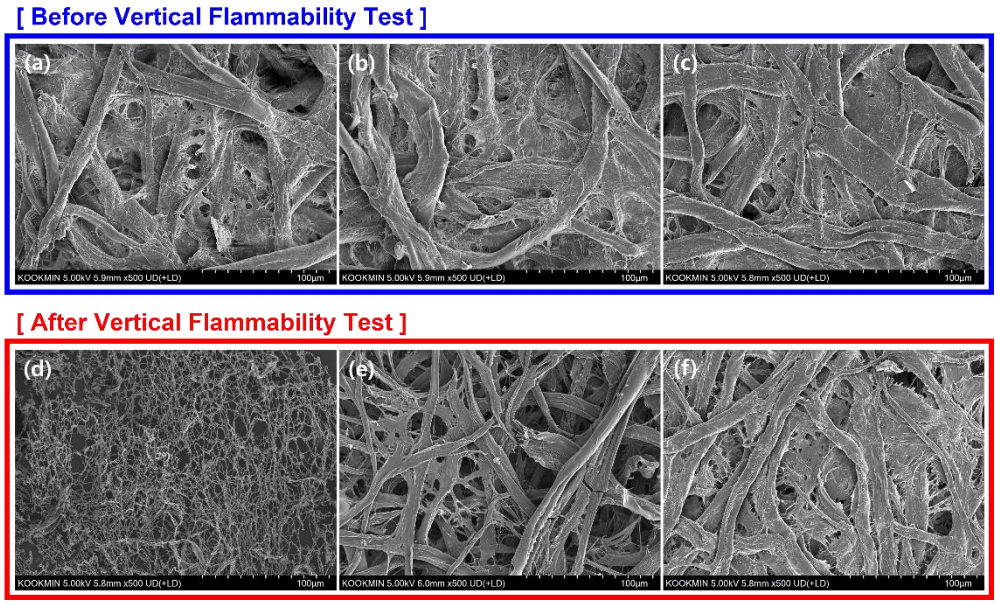

Fig. 7. SEM images of the paper samples: samples (a) C, (b) PS, and (c) LPS before the vertical flammability test and samples (d) C, (e) PS, and (f) LPS after the vertical flammability test

Figure 7(d–f) shows the morphologies of samples C, PS, and LPS after the vertical flammability test. The untreated sample C burned completely, leaving a small amount of ash residue (Fig. 7(d)). In contrast, as shown in Fig. 7(e, f), samples PS and LPS retained their residual carbonized frame after combustion, maintaining their original texture and shape. This structural retention suggests that the thermally stable silica gel formed from sodium silicate effectively stabilized the char layer and improved

the heat shielding properties of the material. In particular, sample LPS (Fig. 7(f)) exhibited the strongest protective effect, primarily attributed to the phosphorylation of lignin. Phosphorus improves the thermal stability of lignin, thereby accelerating dehydration and decarboxylation reactions and increasing the amount of char residue at high temperatures (Prieur *et al*. 2017). It follows that the combined presence of silica gel and phosphorylated lignin contributed to enhanced char formation. In summary, the formation of lignin-silica hybrids not only prevented the release of volatile decomposition products, but also enhances the residual char, which significantly improves the flame-retardant performance of the material.

Thermal Stability Analysis

The TGA curves of paper samples are shown in Fig. 8. This figure compares the weight loss and thermal stability of samples C, PS, and LPS over a temperature range of 0 to 900 °C. The reference sample (sample C) exhibited three stages of thermal decomposition. The first stage, beginning at 40 °C and concluding at 120 °C, is associated with the removal of bound water, whereas the second stage, occurring between 250 and 420 °C, corresponds to the thermal decomposition of wood components, particularly hemicellulose and cellulose (Lin *et al*. 2021). The third stage, occurring between 500 and 600 °C, involves further thermal decomposition of cellulose and other organic compounds.

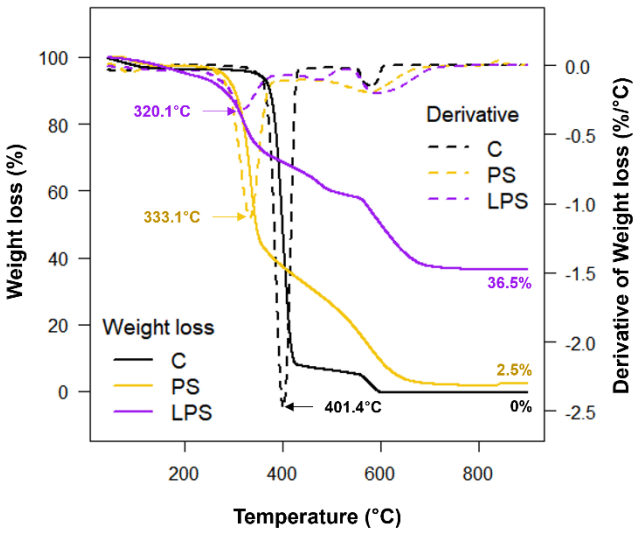

Fig. 8. TGA and DTG curves of C, PS, and LPS

Sample C showed the highest weight loss in the second stage, at 401.4 °C, with a mass residue of 0 wt.% at 900 °C. The addition of flame retardants such as lignin, PA, and sodium silicate to cellulose considerably affected its thermal behavior, which was confirmed by a decrease in the primary decomposition temperature and an increase in the mass of residue. Samples PS and LPS decomposed at 333.1 and 320.1 °C, respectively. This was attributed primarily to the effect of PA, which promotes the formation of dense char at lower temperatures, thereby preventing further thermal decomposition of the material (Patra *et al*. 2020; Mokhena *et al*. 2022). Furthermore, the condensation of phosphate groups leads to the formation of polyphosphate, serving as a protective insulation layer (LeVan 1984). Silica gel acts as a noncombustible inert material, increasing the final char residue (Bahari *et al*. 2019). Notably, the mass of sample LPS stabilizes after decomposition, exhibiting the highest char residue of 36.5 wt.% at 900 °C. Although the spray-coated flame-retardant layer has a relatively low coverage compared to bulk treatments, the synergistic effect of lignin, phytic acid, and

silica gel compensates for this limitation by enabling the formation of a thermally stable, dense char layer. This char effectively insulates the underlying cellulose structure, slowing down thermal degradation and enhancing overall flame resistance. These results support the conclusion that sample LPS possesses the highest thermal stability, explaining its excellent flame-retardant properties.

Flame-Retardant Mechanism and Structure Analysis

Flame-retardant mechanisms of silica and lignin–silica composites

Figure 9(a) shows the mechanism of silica formation from sodium silicate as a precursor in the PS (Lin *et al*. 2023). Silica acts as a physical barrier, suppressing smoldering and flaming combustion by preventing flammable materials from escaping the matrix and preventing the contact of the matrix with O_2 (Rowel 1984). Furthermore, during combustion, P radicals generated from PA effectively scavenge O and H radicals, thereby halting the progression of combustion (Liu *et al*. 2023). Protons derived from PA expedite the dehydration of hydroxyl groups within paper, promoting the formation of char residue. Concurrently, the release of water molecules leads to a reduction in oxygen concentration or partial pressure within the combustion zone. The dehydration of phosphate, leading to the generation of polyphosphate, fosters the formation of protective vitreous layers that impede further combustion (Lin *et al*. 2023).

Figure 9(b) shows the reaction scheme of the formation of lignin–silica hybrids in sample LPS (Zhang *et al*. 2012). The superior flame-retardant properties of sample LPS were attributed to enhanced char formation induced by the lignin–silica composite. In addition, the phosphate group present in PA exhibits remarkable efficacy in diminishing the heat release of lignocellulosic materials.

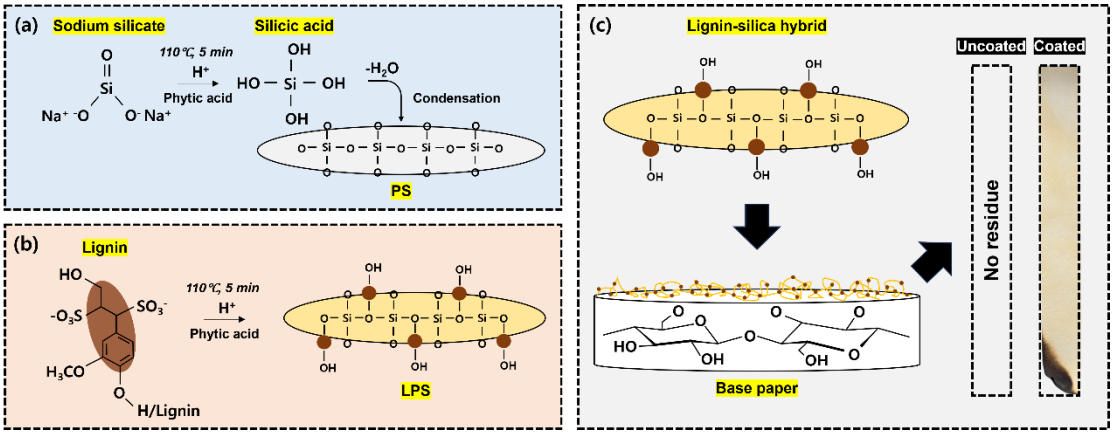

Fig. 9. (a) Mechanism of silica formation, (b) the formation of the lignin–silica hybrids and (c) flame retardancy by spray coating

Elemental Distribution Analysis

Figure 10 exhibits the EDX spectra and elemental maps of samples PS and LPS before and after the vertical flammability test. The surface of samples PS and LPS contained C, O, Na, Si, and P. The elements C and O are mainly derived from cellulose and lignin, and to a lesser extent from PA (Lin *et al*. 2023). P originated from PA. Na and Si mostly originated from sodium silicate. The presence of S and other elements was attributed to kraft pulping, sulfonation, and isolation of lignin.

The O and P contents of sample PS before the vertical flammability test (Fig. 10(a)) are 45.2% and 1.56%, and those in sample LPS (Fig. 10(b)) are 40.6% and 1.86%, respectively. Notably, after the vertical flammability test, samples PS and LPS (Fig. 10(e, f)) exhibit O contents of 13.8% and 20.4% and P contents of 4.35% and 6.40%, respectively. The char residue of these samples mainly consists of phosphoric

complexes enriched with P, O, and aromatic char (Liu *et al*. 2018; Le *et al*. 1997). After the vertical flammability test, the P content of sample LPS was considerably higher than before the vertical flammability test. The dense and rigid carbonized layer observed in Fig. 7(f) and the surface chemical composition in Fig. 10(f, h) indicate that the lignin–silica hybrids modified with PA exerted flame-retardant effect through condensation and gas-phase mechanisms. These results explain the best flame retardancy of sample LPS.

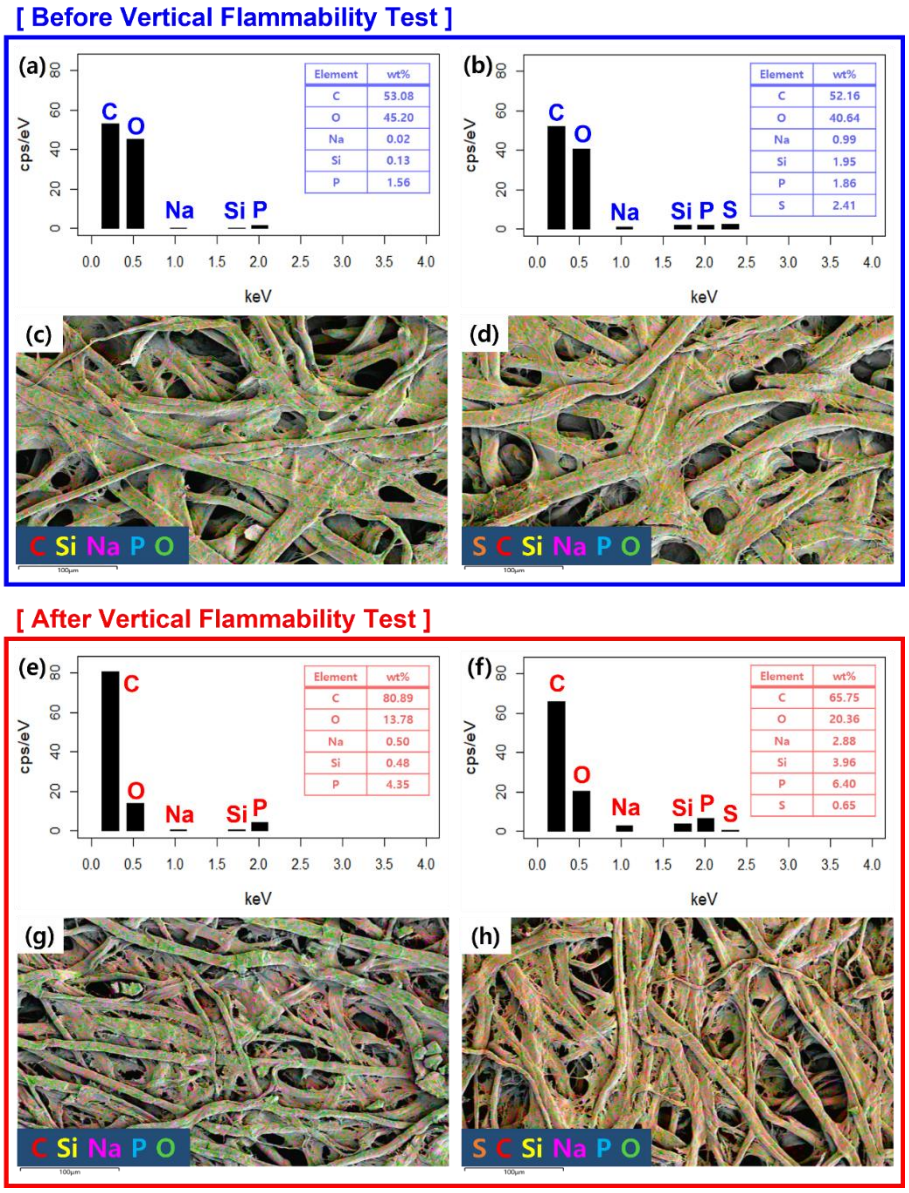

Fig. 10. (a, b, e, and f) EDX spectra and (c, d, g, and h) elemental distribution maps of (a and c) PS before the vertical flammability test, (b and d) LPS before the vertical flammability test, (e and g) PS after the vertical flammability test, and (f and h) LPS after vertical flammability test

Chemical Structure and Residual Char Structure Analysis

The chemical structures of paper samples were characterized *via* ATR-IR analysis (Fig. 11(a, b)). The raw IR spectra (Fig. 11(a)) show a key absorption peak at 1240 cm^{-1}, which was attributed to hydroxyl (–OH) groups and ether (C–O–C) bonds in cellulose (Poletto *et al*. 2012). A peak at 1080 cm^{-1} corresponds to C–O–C bonds present in either lignin or cellulose, and a peak at 935 cm^{-1} is associated with P–O–P

stretching vibrations, indicating the presence of phosphate esters or polyphosphates (Zheng *et al*. 2015). To enhance the resolution and interpretability of the ATR-IR spectra, the raw spectra were processed using the Savitzky–Golay filter (Savitzky and Golay 1964) with a 5th-order polynomial and subjected to second derivative analysis. The processed spectra (Fig. 11(b)) reveal additional absorption peaks that were not as prominent in the original spectrum. These include a peak at 1638 cm^{-1}, corresponding to O–P–O stretching vibrations (Zhang *et al*. 2014), peaks in the range of 1575 to 1450 cm^{-1}, characteristic of the lignin fingerprint region (Reyes and Terrazas 2017), a peak at 1111 cm^{-1} related to Si–O–Si vibrations (Siuda *et al*. 2019; Saleh *et al*. 2020; Sujan *et al*. 2020), and a peak at 1000 cm^{-1} attributed to ether (C–O–C) bonds (Li *et al*. 2020). For pure PA, absorption peaks near 1009 and 891 cm^{-1} correspond to the stretching vibrations of the PO^{-} and P–OH structures (Pan *et al*. 2009; Jiang *et al*. 2012). However, in the spectra of samples coated with PA–silica hybrid, these peaks are not observed, indicating that PA molecules were integrated into the silica network.

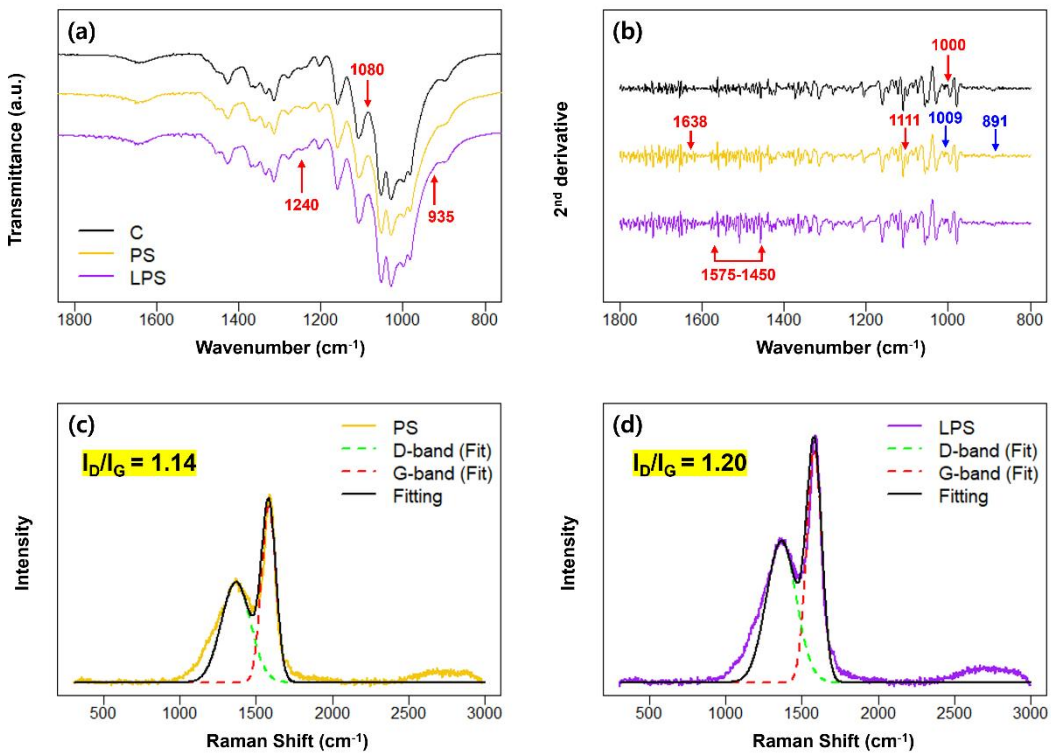

Fig. 11. ATR-IR and Raman spectra of samples C, PS, and LPS: (a) ATR-IR raw spectra, (b) second derivative spectra in the range of 1800 to 800 cm^{-1}, (c) Raman spectra of sample PS after the vertical flammability test, (d) Raman spectra of sample LPS after the vertical flammability test

Raman spectroscopy is an essential tool for characterizing the structure of carbonaceous materials and analyzing the structure of residual char. Therefore, herein, it was used to investigate the mechanisms of the flame-retardant effects (Fig. 11(c, d)). Gaussian fitting was employed for peak analysis (Hou *et al*. 2002; Yu *et al*. 2015), where the G-band at 1574 cm^{-1} represents the organized graphitized structure of the carbon layer, and the D-band at 1354 cm^{-1} corresponds to disordered carbon in the materials. Typically, the ratio of the peak area of the D-band to that of the G-band (I_D/I_G) is used as an indicator of the graphitization degree of residual char (Yu *et al*. 2015). This ratio indicates the microcrystalline size of the carbon layer, with higher values corresponding to smaller carbon structures, improved shielding efficiency, and

enhanced thermal stability. The graphitized char layer acts as a barrier to mass and heat transfer, suppresses the release of volatile organic compounds, and reduces heat release rate during combustion (Hou *et al*. 2002; Yu *et al*. 2015). As shown in Fig. 11(c, d), the introduction of the flame-retardant additives through spray coating enhanced the flame retardancy of paper. The I_D/I_G values of samples PS and LPS are 1.14 and 1.20, respectively. These results suggest that the coating layer stabilized the structure of the residual char, improved the shielding efficiency, and provided a notable flame-retardant effect. This also indicates that the degree of graphitization of the carbon layer was higher in the sample containing lignin. These findings, consistent with the results of the flammability test, SEM-EDX, and TGA, demonstrate that the integration of flame-retardant additives, particularly lignin, significantly enhanced the structural stability and graphitization degree of the residual char, thereby improving thermal shielding and flame-retardant properties.

CONCLUSIONS

1. This study investigated the flame retardancy of cellulose paper enhanced by a composite coating of lignin, phytic acid (PA), and sodium silicate. Through limiting oxygen index (LOI) and vertical flammability tests, significant improvements in fire resistance were confirmed, while scanning electron microscopy (SEM) and attenuated total reflection – infrared (ATR-IR) analyses demonstrated the uniform distribution of flame-retardant additives on the fiber surface. Elemental analysis revealed a notable increase in phosphorus content (from 1.86% to 6.40%) after combustion, indicating the formation of a stable char layer that contributed to enhanced flame resistance.
2. Themogravimetric analysis (TGA) results showed that while the lignin-phytic acid-sodium silicate (LPS) sample began thermal decomposition at a lower temperature compared to other samples, it produced the highest char residue (36.5 wt.%) at 900 °C. This significant char formation was attributed to the synergistic effect of PA, lignin, and sodium silicate, which facilitated the formation of thermally stable silica gel and a dense char layer, effectively insulating the material against heat. Although the LPS sample demonstrated lower initial thermal stability, its superior char yield contributed to enhanced flame resistance. Raman spectroscopy further confirmed the improved graphitization of the char layer in the LPS sample, with an I_D/I_G ratio of 1.20, indicating enhanced shielding efficiency and improved thermal protection.
3. Despite the low coating coverage due to the spray deposition method, the developed flame-retardant system exhibited excellent fire resistance. The synergistic effect between PA, lignin, and silica gel compensated for the limited coating thickness by promoting efficient char formation and thermal insulation. The combined condensed-phase and gas-phase flame-retardant effects, including polyphosphate layer formation and silica gel barrier action, highlight the potential of this eco-friendly and sustainable flame-retardant system for improving the fire resistance of cellulose-based materials, offering promising applications in safety-critical industries. Future research could explore optimizing the coating process for enhanced uniformity and durability, as well as investigating the system's long-term performance under various environmental conditions. Furthermore, this flame-retardant system holds promising potential for industrial applications in safety-critical sectors such as packaging, construction, and textiles, where improved fire resistance is essential.

ACKNOWLEDGMENTS

This study was carried out with the support of 'R&D Program for Forest Science Technology (Project No. 2023473B10-2425-EE02)' provided by Korea Forest Service(Korea Forestry Promotion Institute).

REFERENCES CITED

ASTM D 3801–19 (2019). "Standard test method for measuring the comparative burning characteristics of solid plastics in a vertical position," ASTM International, West Conshohocken, PA, USA.

Bahari, A., Ghovati, M., and Hashemi A. (2019). "Studying of SiO_2/capron nanocomposite as a gate dielectric film for improved threshold voltage," *Applied Physics A* 125(4), 1-7. DOI: 10.1007/s00339-019-2547-3

Bertini, F., Canetti, M., Cacciamani, A., Elegir, G., Orlandi, M., and Zoia, L. (2012). "Effect of ligno-derivatives on thermal properties and degradation behavior of poly(3-hydroxybutyrate)-based biocomposites," *Polymer Degradation and Stability* 97(10), 1979-1987. DOI: 10.1016/j.polymdegradstab.2012.03.009

Chen, Q., Rong, Z., Liu, Z., You, N., and Xie, G. (2021). "Application of modified phytic acid as flame retardant in cellulosic paper," *BioResources* 16(4), 7953-7965. DOI: 10.15376/biores.16.4.7953-7965

Cheng, X. W., Tang, R. C., and Guan, J. P. (2020). "An eco-friendly and effective flame retardant coating for cotton fabric based on phytic acid doped silica sol approach," *Progress in Organic Coatings* 141, article 105539. DOI: 10.1016/j.porgcoat.2020.105539

Costes, L., Laoutid, F., Brohez, S., Delvosalle, C., and Dubois, P. (2017). "Phytic acid–lignin combination: A simple and efficient route for enhancing thermal and flame retardant properties of polylactide," *European Polymer Journal* 94, 270-285. DOI: 10.1016/j.eurpolymj.2017.07.018

Fan, L., Zhang, Y., Liu, S., Zhou, N., Chen, P., Cheng, Y., Addy, M., Lu, Q., Omar, M. M., Liu, Y., Wang, Y., Dai, L., Anderson, E., Peng, P., Lei, H., and Ruan, R. (2017). "Bio-oil from fast pyrolysis of lignin: Effects of process and upgrading parameters," *Bioresource Technology* 241, 1118-1126. DOI: 10.1016/j.biortech.2017.05.129

Ferry, L., Dorez, G., Taguet, A., Otazaghine, B., and Lopez-Cuesta, J. M. (2015). "Chemical modification of lignin by phosphorus molecules to improve the fire behavior of polybutylene succinate," *Polymer Degradation and Stability* 113, 135-143. DOI: 10.1016/j.polymdegradstab.2014.12.015

Figueiredo, J. A., Ismael, M. I., Anjo, C. M., and Duarte, A. P. (2010). "Cellulose and derivatives from wood and fibers as renewable sources of raw materials," *Topics in Current Chemistry* 294, 117-128. DOI: 10.1007/128_2010_88

Graf, E., and Eaton, J. W. (1990). "Antioxidant functions of phytic acid," *Free Radical Biology and Medicine* 8, 61-69. DOI: 10.1016/0891-5849(90)90146-A

Hou, F., Zhu, M., Liu, Y., Zhu, K., Xu, J., Jiang, Z., Wang, C., and Wang, H. (2022). "A self-assembled bio-based coating with phytic acid and DL-arginine used for a flame-retardant and antibacterial cellulose fabric," *Progress in Organic Coatings* 173, article 107179. DOI: 10.1016/j.porgcoat.2022.107179

IEC 60695-11-10 (2013). "Fire hazard testing - Part 11-10: Test flames - 50 W horizontal and vertical flame test methods," International Electrotechnical Commission, Geneva, Switzerland.

Jeong, S. H., Park, C. H., Song, H., Heo, J. H., and Lee, J. H. (2022). "Biomolecules

as green flame retardants: Recent progress, challenges, and opportunities," *Journal of Cleaner Production* 368. DOI: 10.1016/j.jclepro.2022.133241

Jiang, G., Qiao, J., and Hong, F. (2012). "Application of phosphoric acid and phytic acid-doped bacterial cellulose as novel proton-conducting membranes to PEMFC," *International Journal of Hydrogen Energy* 37(11), 9182-9192. DOI: 10.1016/j.ijhydene.2012.02.195

Kalia, S., Avérous, L., Njuguna, J., Dufresne, A., and Cherian, B. M. (2011). "Natural fibers, bio- and nanocomposites," *International Journal of Polymer Science* 2011, 1-2. DOI: 10.1155/2011/735932

Katović, D., Bischof-Vukušić, S., Flinčec-Grgac, S., Lozo, B., and Banić, D. (2009). "Flame retardancy of paper obtained with environmentally friendly agents," *Fire and Europe, Technical Innovations in Environmental Managemen*t 17(3), 74, 90-94.

Köklükaya, O., Carosio, F., Grunlan, J. C., and Wågberg, L. (2015). "Flame-retardant paper from wood fibers functionalized via layer-by-layer assembly," *ACS Applied Materials and Interfaces* 7(42), 23750-23759. DOI: 10.1021/acsami.5b08105

Kong, F. B., He, Q. L., Peng, W., Nie, S. B., Dong, X., and Yang, J. N. (2020). "Eco-friendly flame retardant poly(lactic acid) composites based on banana peel powders and phytic acid: Flame retardancy and thermal property," *Journal of Polymer Research* 27(8), 1-12. DOI: 10.1007/s10965-020-02176-4

Laftah, W. A., and Wan Abdul Rahman, W. A. (2016). "Pulping process and the potential of using non-wood pineapple leaves fiber for pulp and paper production: A review," *Journal of Natural Fibers* 13(1), 85-102. DOI: 10.1080/15440478.2014.984060

Le, B. M., Bourbigot, S., Le, T. Y., and Laureyns, J. (1997). "Synergy in intumescence—Application to β-cyclodextrin carbonisation agent in intumescent additives for fire retardant polyethylene formulations," *Polymer Degradation and Stability* 56(1), 11-21. DOI: 10.1016/S0141-3910(96)00190-5

LeVan, S. L. (1984). "Chemistry of fire retardancy," in: *The Chemistry of Solid Wood*, R. Rowell (ed.), American Chemical Society, Washington, D.C., pp. 531-574. DOI: 10.1021/ba-1984-0207.ch014

Li, P., Sirviö, J. A., Hong, S., Ämmälä, A., and Liimatainen, H. (2019). "Preparation of flame-retardant lignin-containing wood nanofibers using a high-consistency mechano-chemical pretreatment," *Chemical Engineering Journal* 375. DOI: 10.1016/j.cej.2019.122050

Li, P., Zhang, Y., Zuo, Y., Lu, J., Yuan, G., and Wu, Y. (2020). "Preparation and characterization of sodium silicate impregnated Chinese fir wood with high strength, water resistance, flame retardant and smoke suppression," *Journal of Materials Research and Technology* 9(1), 1043-1053. DOI: 10.1016/j.jmrt.2019.10.035

Lin, C. F., Karlsson, O., Martinka, J., Rantuch, P., Garskaite, E., Mantanis, G. I., Jones, D., and Sandberg, D. (2021). "Approaching highly leaching-resistant fire-retardant wood by in situ polymerization with melamine formaldehyde resin," *ACS Omega* 6(19), 12733-12745. DOI: 10.1021/acsomega.1c01044

Lin, C. F., Zhang, C., Karlsson, O., Martinka, J., Mantanis, G. I., Rantuch, P., Jones, D., and Sandberg, D. (2023). "Phytic acid-silica system for imparting fire retardancy in wood composites," *Forests* 14(5). DOI: 10.3390/f14051021

Liu, X., Lei, C., and Fang, Y. (2022). "Fully bio-based chitosan/sodium alginate coating for flame retardant Xuan paper," *BioResources* 17(4), 6521-6531. DOI: 10.15376/biores.17.4.6521-6531

Liu, X. H., Zhang, Q. Y., Cheng, B. W., Ren, Y. L., Zhang, Y. G., and Ding, C. (2018). "Durable flame retardant cellulosic fibers modified with novel, facile and

efficient phytic acid-based finishing agent," *Cellulose* 25(1), 799-811. DOI: 10.1007/s10570-017-1550-0

Liu, Y., Zhang, A., Cheng, Y., Li, M., Cui, Y., and Li, Z. (2023). "Recent advances in biomass phytic acid flame retardants," *Polymer Testing* 124. DOI: 10.1016/j.polymertesting.2023.108100

Martinka, J., Mantanis, G. I., Lykidis, C., Antov, P., and Rantuch, P. (2022). "The effect of partial substitution of polyphosphates by aluminium hydroxide and borates on the technological and fire properties of medium density fibreboard," *Wood Material Science and Engineering* 17(6), 720-726. DOI: 10.1080/17480272.2021.1933175

Mokhena, T. C., Sadiku, E. R., Ray, S. S., Mochane, M. J., Matabola, K. P., and Motloung, M. (2022). "Flame retardancy efficacy of phytic acid: An overview," *Journal of Applied Polymer Science* 139(27), e52495. DOI: 10.1002/app.52495

Mousavioun, P., Doherty, W. O. S., and George, G. (2010). "Thermal stability and miscibility of poly(hydroxybutyrate) and soda lignin blends," *Industrial Crops and Products* 32(3), 656-661. DOI: 10.1016/j.indcrop.2010.08.001

Nassar, M. M., Fadali, O. A., Khattab, M. A., and Ashour, E. A. (1999). "Thermal studies on paper treated with flame-retardant," *Fire and Materials* 23(3), 125-129. DOI:10.1002/(SICI)1099-1018(199905/06)23:3<125::AID-FAM677>3.0.CO;2-X

Ni, J., Chen, L., Zhao, K., Hu, Y., and Song, L. (2011). "Preparation of gel-silica/ammonium polyphosphate core-shell flame retardant and properties of polyurethane composites," *Polymers for Advanced Technologies* 22(12), 1824-1831. DOI: 10.1002/pat.1679

Niu, M., Hagman, O., Wang, A., Xie, Y., Karlsson, O., and Cai, L. (2014). "Effect of Si-Al compounds on fire properties of ultra-low density fiberboard," *BioResources* 9(2), 2415-2430. DOI: 10.5555/20143186967

Pan, F., Yang, X., and Zhang, D. (2009). "Chemical nature of phytic acid conversion coating on AZ61 magnesium alloy," *Applied Surface Science* 255(20), 8363-8371. DOI: 10.1016/j.apsusc.2009.05.089

Patra, A., Kjellin, S., and Larsson, A. C. (2020). "Phytic acid-based flame retardants for cotton," *Green Materials* 8(3), 123-130. DOI: 10.1680/jgrma.19.00054

Poletto, M., Zattera, A. J., and Santana, R. M. C. (2012). "Structural differences between wood species: Evidence from chemical composition, FTIR spectroscopy, and thermogravimetric analysis," *Journal of Applied Polymer Science* 126(S1), E337-E344. DOI: 10.1002/app.36991

Prieur, B., Meub, M., Wittemann, M., Klein, R., Bellayer, S., Fontaine, G., and Bourbigot, S. (2017). "Phosphorylation of lignin: Characterization and investigation of the thermal decomposition," *RSC Advances* 7(27), 16866-16877. DOI: 10.1039/C7RA00295E

Reddy, N. R., Sathe, S. K., and Salunkhe, D. K. (1982). "Phytates in legumes and cereals," *Advances in Food Research* 28, 1-92. DOI: 10.1016/S0065-2628(08)60110-X

Reyes-Rivera, J., and Terrazas, T. (2017). "Lignin analysis by HPLC and FTIR," *Methods in Molecular Biology* 1544, 193-211. DOI: 10.1007/978-1-4939-6722-3_14

Rowell, R. (1984). *The Chemistry of Solid Wood*, American Chemical Society, Washington, D.C.

Saba, N., Jawaid, M., Paridah, M. T., and Al-Othman, O. Y. (2016). "A review on flammability of epoxy polymer, cellulosic and non-cellulosic fiber reinforced epoxy composites," *Polymers for Advanced Technologies* 27(5), 577-590. DOI: 10.1002/pat.3739

Saleh, T. A., Baig, N., Alghunaimi, F. I., and Aljuryyed, N. W. (2020). "A flexible

biomimetic superhydrophobic and superoleophilic 3D macroporous polymer-based robust network for the efficient separation of oil-contaminated water," *RSC Advances* 10(9), 5088-5097. DOI: 10.1039/C9RA06579B

Savitzky, A., and Golay, M. J. E. (1964). "Smoothing and differentiation of data by simplified least squares procedures," *Analytical Chemistry* 36(8), 1627-1639. DOI: 10.1021/ac60214a047

Schlomach, J., and Kind, M. (2004). "Investigations on the semi-batch precipitation of silica," *Journal of Colloid and Interface Science* 277(2), 316-326. DOI: 10.1016/j.jcis.2004.04.051

Siuda, J., Perdoch, W., Mazela, B., and Zborowska, M. (2019). "Catalyzed reaction of cellulose and lignin with methyltrimethoxysilane-FT-IR, 13C NMR and 29Si NMR studies," *Ma*terials 12(12), article 2006. DOI: 10.3390/ma12122006

Song, P., Cao, Z., Fu, S., Fang, Z., Wu, Q., and Ye, J. (2011). "Thermal degradation and flame retardancy properties of ABS/lignin: Effects of lignin content and reactive compatibilization," *Thermochimica Acta* 518(1-2), 59-65. DOI: 10.1016/j.tca.2011.02.007

Sujan, M. I., Sarkar, S. D., Sultana, S., Bushra, L., Tareq, R., Roy, C. K., and Azam, M. S. (2020). "Bi-functional silica nanoparticles for simultaneous enhancement of mechanical strength and swelling capacity of hydrogels," *RSC Advances* 10(11), 6213-6222. DOI: 10.1039/C9RA09528D

Xu, F., Zhong, L., Xu, Y., Feng, S., Zhang, C., Zhang, F., and Zhang, G. (2019). "Highly efficient flame-retardant kraft paper," *Journal of Materials Science* 54(2), 1884-1897. DOI: 10.1007/s10853-018-2911-2

Yang, H., Yu, B., Xu, X., Bourbigot, S., Wang, H., and Song, P. (2020). "Lignin-derived bio-based flame retardants toward high-performance sustainable polymeric materials," *Green Chemistry* 22(7), 2129-2161. DOI: 10.1039/D0GC00449A

Yu, B., Shi, Y., Yuan, B., Qiu, S., Xing, W., Hu, W., Song, L., Lo, S., and Hu, Y. (2015). "Enhanced thermal and flame retardant properties of flame-retardant-wrapped graphene/epoxy resin nanocomposites," *Journal of Materials Chemistry A* 3(15), 8034-8044. DOI: 10.1039/C4TA06613H

Yuan, H. B., Tang, R. C., and Yu, C. B. (2021). "Flame retardant functionalization of microcrystalline cellulose by phosphorylation reaction with phytic acid," *International Journal of Molecular Sciences* 22(17), article 9631. DOI: 10.3390/ijms22179631

Zhang, R., Xiao, X., Tai, Q., Huang, H., Yang, J., and Hu, Y. (2012). "Preparation of lignin–silica hybrids and its application in intumescent flame-retardant poly(lactic acid) system," *High Performance Polymers* 24(8), 738-746. DOI: 10.1177/0954008312451476

Zhang, S., Li, S. N., Wu, Q., Li, Q., Huang, J., Li, W., Zhang, W., and Wang, S. (2021). "Phosphorus containing group and lignin toward intrinsically flame retardant cellulose nanofibril-based film with enhanced mechanical properties," *Composites Part B: Engineering* 212, article 108699. DOI: 10.1016/j.compositesb.2021.108699

Zhang, T., Yan, H., Shen, L., Fang, Z., Zhang, X., Wang, J., and Zhang, B. (2014). "Chitosan/phytic acid polyelectrolyte complex: A green and renewable intumescent flame retardant system for ethylene-vinyl acetate copolymer," *Industrial and Engineering Chemistry Research* 53(49), 19199-19207. DOI: 10.1021/ie503421f

Zheng, C., Li, D., and Ek, M. (2019). "Improving fire retardancy of cellulosic thermal insulating materials by coating with bio-based fire retardants," *Nordic Pulp and Paper Research Journal* 34(1), 96-106. DOI: 10.1515/npprj-2018-0031

Zheng, Z., Liu, S., Cui, X., Wang, H., Cui, X., and Wang, H. (2015). "Preparation of a novel phosphorus- and nitrogen-containing flame retardant and its synergistic effect in the intumescent flame-retarding polypropylene system," *Polymer Composites* 36(9), 1606-1619. DOI: 10.1002/pc.23069

Article submitted: February 10, 2025; Peer review completed: March 1, 2025;
Revised version received and accepted: March 12, 2025; Published: April 3, 2025;
DOI: 10.15376/biores.20.2.3808-3825